JOURNAL OF MATERIALS SCIENCE 31 (1996) 2159–2164

Incorporation of $LiNbO_3$ crystals into tellurite glasses

HYUN GYU KIM, TAKAYUKI KOMATSU, RYUJI SATO, KAZUMASA MATUSITA
Department of Chemistry, Nagaoka University of Technology, Kamitomioka-cho, Nagaoka 940-21, Japan

Transparent tellurite glasses containing 5–10 μm diameter $LiNbO_3$ crystals (3–7 wt%) have been successfully prepared using an incorporation method in which $LiNbO_3$ crystals are directly dispersed into the $80TeO_2$–$15Li_2O$–$5Nb_2O_5$ glass. The dissolution behaviour of the $LiNbO_3$ crystals greatly depends on the Li_2O: Nb_2O_5 ratio in the matrix glasses. In the $80TeO_2$–$10Li_2O$–$10Nb_2O_5$ matrix glass, the crystals remaining after incorporation have the composition $LiNb_3O_8$. A small difference in the refractive indices, *n*, between the TeO_2-based glasses ($n = 2.07$) and the incorporated $LiNbO_3$ crystals ($n = 2.296$) is a significant reason for the transparency. It is feasible to prepare the highly transparent TeO_2-based glasses containing a large amount of $LiNbO_3$ crystals by controlling the incorporation process.

1. Introduction

Recently the present authors [1] succeeded in preparing transparent tellurite glasses containing 10 μm diameter $LiNbO_3$ crystals by using a two-step heat-treatment process for the glasses based on the TeO_2–Li_2O–Nb_2O_5 system. Such glasses are candidates for nonlinear optical applications. The favourite glass composition for the precipitation of $LiNbO_3$ crystals was $50TeO_2$–$35Li_2O$–$15Nb_2O_5$ with a high Li^+:Nb^{5+} ratio [1]. Recently transparent tellurite glasses containing $KNbO_3$ crystals have also been fabricated using an incorporation method in which the $KNbO_3$ particles are directly incorporated into the TeO_2–K_2O–Nb_2O_5 glasses [2]. An incorporation method has an advantage of the choice of matrix glass composition as compared to a crystallization method. In addition it is easy to form glasses created by the incorporation method into desired shapes such as fibres. The reason that TeO_2-based glasses are used as matrix glasses is that the refractive indices of the TeO_2-based glasses and many ferroelectric materials are similar which leads to extremely low scattering losses at the glass/crystal interface [1–4]. In addition, it should be noted that tellurite glasses have low melting temperatures and good infrared transmissions [5, 6] and are also promising materials for use in nonlinear optical devices [7, 8]. The preparation and optical properties of TeO_2-based glasses containing ferroelectrics, is therefore, of particular interest.

In this study, we fabricate transparent TeO_2–Li_2O–Nb_2O_5 glasses containing 10 μm diameter $LiNbO_3$ crystals using an incorporation method. The solubility behaviours of the $LiNbO_3$ crystals in the tellurite glasses, particularly the effects of the matrix glass composition, the incorporation temperature and melting time have on the solubility, have been clarified.

2. Experimental

The nominal compositions examined in the present study were $80TeO_2$–$(20 - x)Li_2O$–xNb_2O_5 ($x = 5, 8$ and 10 mol%). The bulk glasses were prepared by using a conventional melt-quenching method. The raw materials used were reagent grade TeO_2 (99%, Soekawa Chemicals), Li_2CO_3 (99%, Nacalai Tesque) and Nb_2O_5 (99.9%, Soekawa Chemicals). Batches of 30 g size were melted in a platinum crucible at 900–950 °C for 60 min in an electric furnace. The $LiNbO_3$ powder (99.9%, Aldrich Chemicals) was calcined at 800 °C for 24 h and sintered at 1170 °C for 6 h in order to develop the particle size. The presence of $LiNbO_3$ crystals as a single phase in the sintered ceramics was confirmed from the X-ray diffraction (XRD) analysis.

The TeO_2–Li_2O–Nb_2O_5 glasses and sintered $LiNbO_3$ ceramics were pulverized, and then were intimately mixed. The grain size of the $LiNbO_3$ powders was less than 37 μm. The mixtures were heated in a platinum crucible at 700–1000 °C. After stirring with a silica glass rod and holding for several minutes, the remelted samples were poured on to an iron plate. The XRD experiments performed at room temperature using Cu*K*α radiation verified the presence of $LiNbO_3$ crystals in the glasses. The transparency of the remelted samples was checked through optical spectra. The refractive index, *n*, of glasses for a wavelength of 632.8 nm (He–Ne laser) at room temperature was measured using an ellipsometer (Model DVA-36L, Mizojiri Optical Co.). The size and dispersion state of the $LiNbO_3$ crystals in the matrix glasses were examined with an optical polarization microscope.

3. Results

The DTA curves of $80TeO_2$–$10Li_2O$–$10Nb_2O_5$ and $80TeO_2$–$15Li_2O$–$5Nb_2O_5$ glasses are shown in Fig. 1.

0022–2461 © *1996 Chapman & Hall*

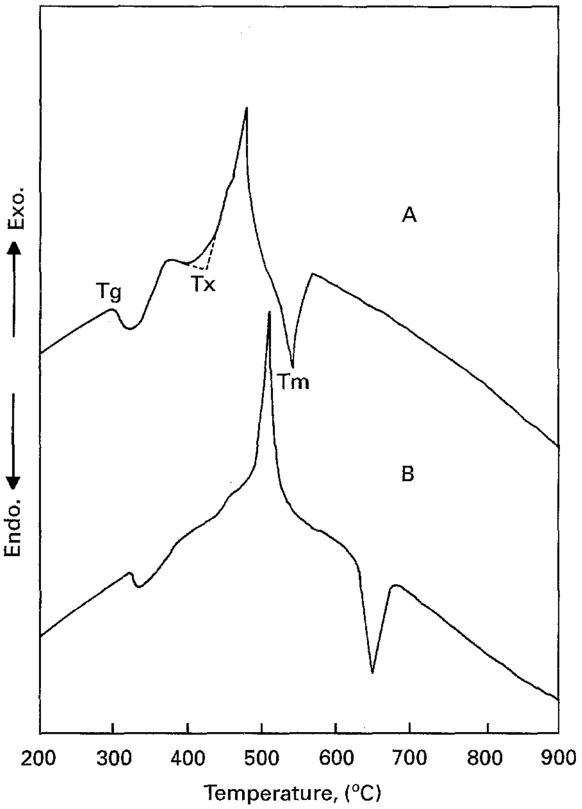

Figure 1 DTA curves for tellurite glasses. The heating rate was 10 °C min^{-1}. A: $80TeO_2$–$15Li_2O$–$5Nb_2O_5$, B: $80TeO_2$–$10Li_2O$–$10Nb_2O_5$.

The values of the glass transition, T_g, crystallization onset, T_x, and melting, T_m, temperatures for the $80TeO_2$–$15Li_2O$–$5Nb_2O_5$ glass are 303, 473, and 550 °C, respectively. The numerical difference between T_g and T_x, ($\Delta T = T_x – T_g$), in this glass is 170 °C, indicating that the thermal stability of this glass is extremely high. The values of T_g, T_x and T_m for the glasses examined in this study are summarized in Table I, together with the values of refractive index, n, and density, ρ. All glasses are transparent and yellowish.

Fig. 2 shows the room temperature XRD patterns for the samples obtained by remelting a mixture of the powders of $80TeO_2$–$(20 - x)Li_2O$–xNb_2O_5 glasses and $LiNbO_3$ crystals at 950 °C for 1 min, where the added amount of $LiNbO_3$ crystals was 15 wt %. In the matrix glass of $80TeO_2$–$10Li_2O$–$10Nb_2O_5$ composition, the XRD pattern indicates the presence of $LiNb_3O_8$ crystals. It is very strange that the presence of $LiNbO_3$ crystals is not confirmed, although $LiNbO_3$ crystals were incorporated into the glass. In the matrix glass of $80TeO_2$–$12Li_2O$–$8Nb_2O_5$ composition, the presence of both $LiNbO_3$ and $LiNb_3O_8$ crystals is confirmed. In the matrix glass of $80TeO_2$–$15Li_2O$–$5Nb_2O_5$ composition, only the XRD peaks attributable to $LiNbO_3$ crystals are observed. These results indicate that the crystalline phase present in the remelted samples implicitly depends on the composition of the matrix glasses, i.e. on the ratio $Li_2O:Nb_2O_5$. In addition the results indicate that TeO_2–Li_2O–Nb_2O_5 glasses with high $Li_2O:Nb_2O_5$ ratios are favourable for the incorporation of $LiNbO_3$ crystals.

TABLE I Values of glass transition temperature, T_g, crystallization onset temperature, T_x, melting temperature, T_m, refractive index, n, and density, ρ, for $80TeO_2$–$(20 - x)Li_2O$–xNb_2O_5 glasses.

Glass	T_g (°C)	T_x (°C)	T_m (°C)	n	ρ (g cm^{-3})
x = 5	303	473	550	2.07	5.06
x = 8	318	487	614	2.08	5.11
x = 10	326	496	663	2.09	5.16

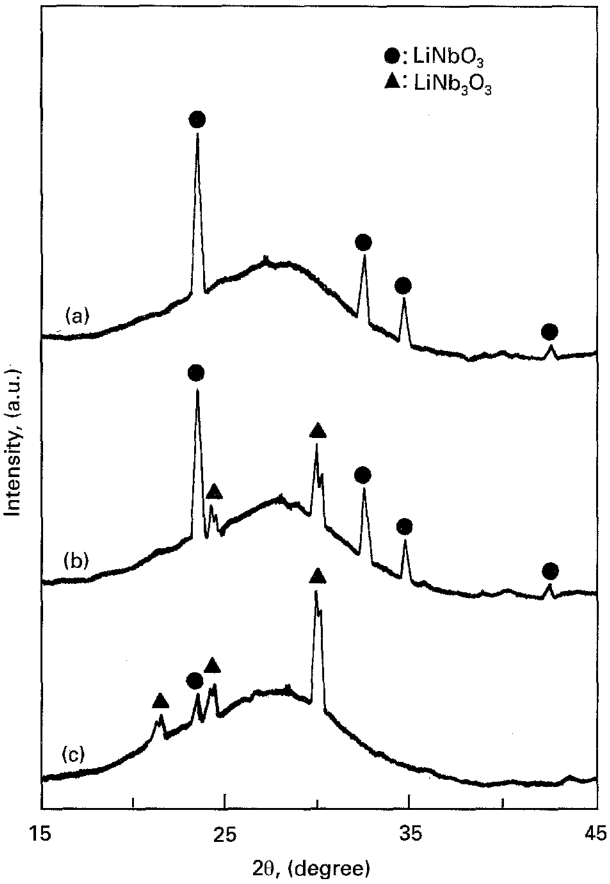

Figure 2 Powder XRD patterns (Cu K_α) at room temperature for the samples obtained by remelting the mixtures of the powders of $80TeO_2$–$(20 - x)Li_2O$–xNb_2O_5 glasses and 15 wt % $LiNbO_3$ crystals for (a) $x = 5$, (b) $x = 8$ and (c) $x = 10$. The remelting temperature and time were 950 °C and 1 min, respectively.

Fig. 3 shows the XRD patterns at room temperature for the samples obtained by remelting a mixture of the powders of $80TeO_2$–$15Li_2O$–$5Nb_2O_5$ glass and $LiNbO_3$ crystals (15 wt %) at 950 °C for 1, 1.5 and 2 min. For the sample remelted for 2 min, no crystalline peaks are detected, indicating the perfect dissolution of the $LiNbO_3$ crystals into the matrix glass. For the sample remelted for 1.5 min, the XRD pattern clearly indicates the presence of $LiNbO_3$ crystals. The optical photographs for these remelted samples are shown in Fig. 4. A sample remelted for 40 s is black and opaque. The samples remelted for 1 and 1.5 min, however, are transparent. The optical polarization micrograph for the sample remelted for 1.5 min is shown in Fig. 5. $LiNbO_3$ crystals with diameters of about 5–10 μm are dispersed in the matrix glass. The optical absorption spectra for these melted samples are shown in Fig. 6. The absorption edge energies, E_g,

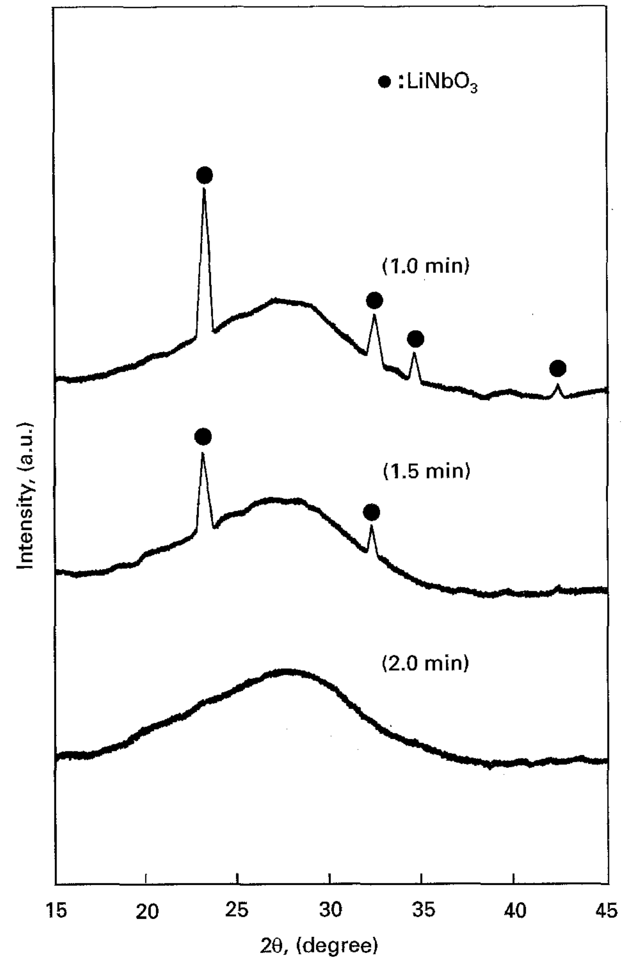

Figure 3 Powder XRD patterns (Cu*K*α) at room temperature for the samples obtained by remelting the mixtures of the powders of $80TeO_2$–$15Li_2O$–$5Nb_2O_5$ glass and $LiNbO_3$ cyrstals (15 wt %). The remelting temperature was 950 °C.

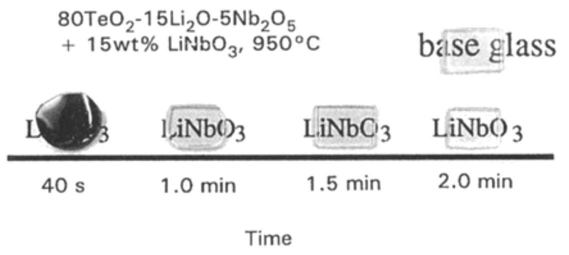

Figure 4 Optical photographs for the samples obtained by remelting the mixtures of the powders of $80TeO_2$–$15Li_2O$–$5Nb_2O_5$ glass and $LiNbO_3$ crystals (15 wt %). The remelting temperature was 950 °C.

for the samples are almost the same, i.e. $E_g = 3.18$ eV (390 nm), and the transmittance at wavelengths above 400 nm increases with increasing remelting time. We note that the $LiNbO_3$ crystals with $E_g = 3.54$ eV (350 nm) are colourless above 400 nm [9].

In order to check the dissolution process of the $LiNbO_3$ crystals into the $80TeO_2$–$15Li_2O$–$5Nb_2O_5$ glass, a thermal analysis for the mixture of $80TeO_2$–$15Li_2O$–$5Nb_2O_5$ glass powder and $LiNbO_3$ crystalline powder (15 wt %) was performed. The DTA curve taken for this mixture is shown in Fig. 7. It is seen that the value of T_g and T_x for the mixture are almost the same as those for the matrix glass

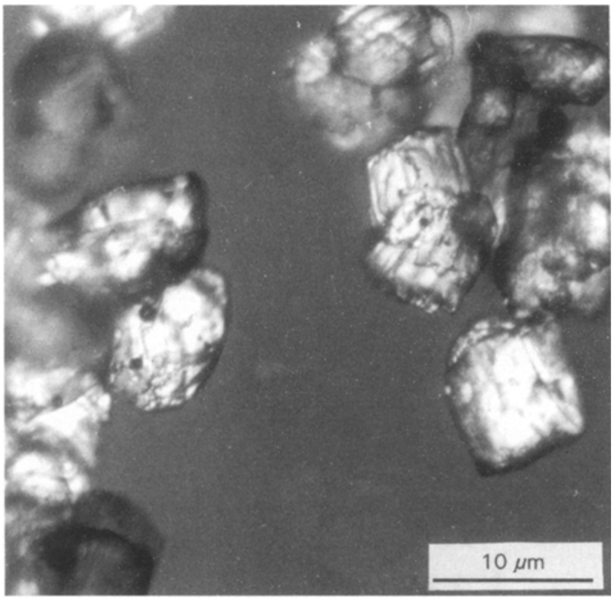

Figure 5 Polarization microscope photograph for the sample obtained by remelting the mixture of the powders of $80TeO_2$–$15Li_2O$–$5Nb_2O_5$ glass and $LiNbO_3$ crystals (15 wt %). The remelting temperature and time was 950 °C and 1.5 min, respectively.

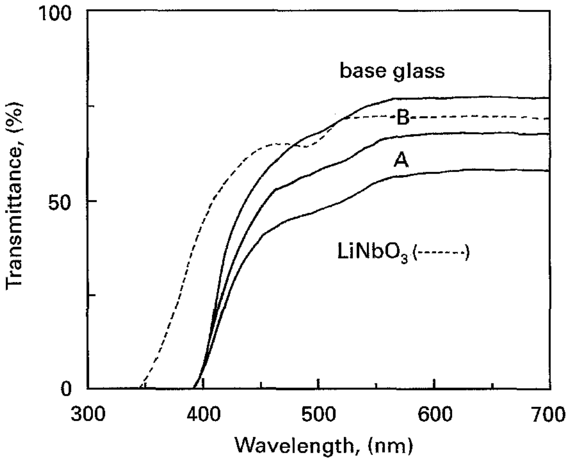

Figure 6 Optical transmittance spectra for the samples obtained by remelting the mixtures of the powders of $80TeO_2$–$15Li_2O$–$5Nb_2O_5$ glass and $LiNbO_3$ crystals (15 wt %). A: the sample remelted at 950 °C for 1 min, B: the sample remelted at 950 °C for 1.5 min.

containing no $LiNbO_3$ crystals. However, for the mixed sample, two endothermic peaks are clearly observed. From comparison with the DTA curve obtained for the pure matrix glass, it is concluded that the first endothermic peak appearing at around 540 °C is the same as in Fig. 1. The second endothermic peak appearing at around 680 °C is then due to the dissolution of $LiNbO_3$ crystals into the matrix melt.

In the incorporation method, the estimation of the amount of $LiNbO_3$ crystals remaining in the transparent glass is one of the most important points. Fig. 8 shows a schematic of the room temperature XRD pattern for the mixture of the $80TeO_2$–$15Li_2O$–$5Nb_2O_5$ glass powder and $LiNbO_3$ crystalline powder. The ratio of the $LiNbO_3$ (012) plane peak area, S_c, to the halo pattern area, S_g, due to the matrix glass, S_c: S_g is shown in Fig. 9 as a function of the content of $LiNbO_3$

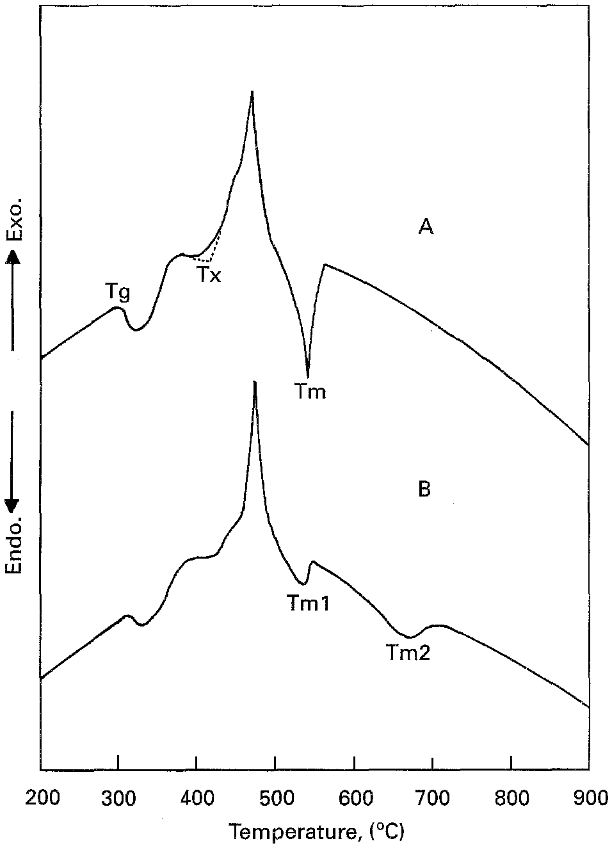

Figure 7 DTA curves for the tellurite glasses powders. The heating rate was 10 °C min^{-1}. A: 80TeO$_2$–15Li$_2$O–5Nb$_2$O$_5$, B: 80TeO$_2$–15Li$_2$O–5Nb$_2$O$_5$ + 15 wt % LiNbO$_3$.

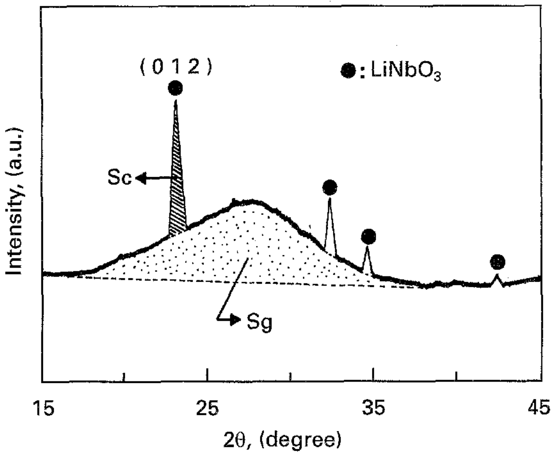

Figure 8 Powder XRD patterns (Cu*K*α) at room temperature for the mixture of the powders of 80TeO$_2$–15Li$_2$O–5Nb$_2$O$_5$ and LiNbO$_3$ crystals (15 wt %). S_c is the peak area due to the (012) plane of LiNbO$_3$ crystals, and S_g is the area of the halo due to the glass.

crystals. A linear correlation between the ratio of S_c: S_g and the added amount of LiNbO$_3$ crystals is observed. It is found that the amount of LiNbO$_3$ crystals present in the samples produced by the remelting for 1 and 1.5 min of a mixture of 80TeO$_2$–15Li$_2$O–5Nb$_2$O$_5$ glass and 15 wt % of LiNbO$_3$ crystals are about 7 and 3 wt %, respectively, as shown in Fig. 9. The amount of LiNbO$_3$ crystals present in the samples remelted at various temperatures for 1, 1.5 and 2 min are presented in Fig. 10. It is seen that at temperatures above 700 °C the LiNbO$_3$ crystals dissolve rapidly into the

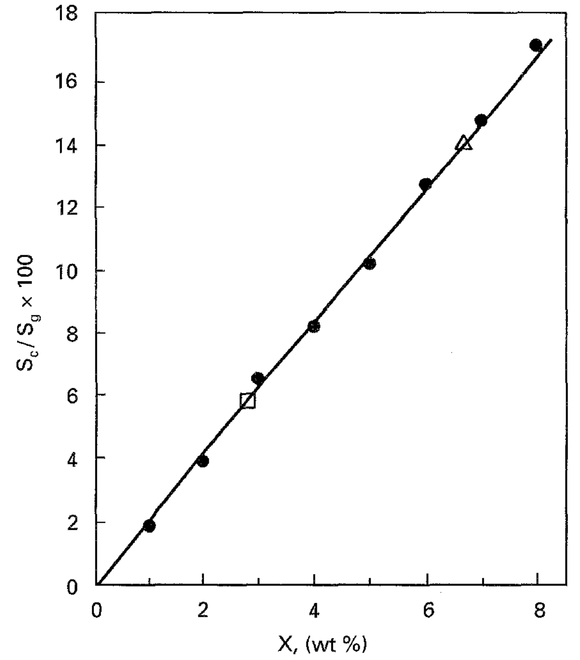

Figure 9 Correlation between the values of S_c/S_g in XRD patterns (●) and the amount of LiNbO$_3$ crystals in the mixtures of 80TeO$_2$–15Li$_2$O–5Nb$_2$O$_5$ glass and LiNbO$_3$ crystals. The values of S_c/S_g for the remelted samples of the mixtures of 80TeO$_2$–15Li$_2$O–5Nb$_2$O$_5$ glass and LiNbO$_3$ crystals (15 wt %) at 950 °C for 1 min (△) and 1.5 min (□) are also shown.

80TeO$_2$–15Li$_2$O–5Nb$_2$O$_5$ glass. These results support the assignment that the endothermic peak at around 680 °C shown in Fig. 7 is due to the dissolution of the LiNbO$_3$ crystals into the glass melt.

4. Discussion

4.1. Effect of the matrix glass composition on LiNbO$_3$ incorporation

One of the most striking results obtained in the present study is that the crystalline phase present in the remelted samples of the mixtures of TeO$_2$–Li$_2$O–Nb$_2$O$_5$ glass and 15 wt % LiNbO$_3$ crystals changes with the ratio of Li$_2$O:Nb$_2$O$_5$ in the matrix glass. For example, the crystalline phase present in the remelted sample of a mixture of 80TeO$_2$–10Li$_2$O–10Nb$_2$O$_5$ glass and LiNbO$_3$ crystals is not LiNbO$_3$ but LiNb$_3$O$_8$, as is shown in Fig. 2. In the Li$_2$O–Nb$_2$O$_5$ binary phase diagram [10], the LiNb$_3$O$_8$ phase exists over a wide composition range of the Nb$_2$O$_5$-rich side. It is obvious that the behaviour of Li$^+$ in the matrix glasses and in the LiNbO$_3$ crystals is important for the phase transformation of LiNbO$_3$ to LiNbO$_3$O$_8$ during the remelting. It is worth noting the effect of the glass composition has on the crystallization of the LiNbO$_3$ crystals from TeO$_2$–Li$_2$O–Nb$_2$O$_5$ glasses [1]. In the previous paper [1], we demonstrated that LiNbO$_3$ crystals were directly precipitated from the 50TeO$_2$–35Li$_2$O–15Nb$_2$O$_5$ glass with a high Li$^+$ content and thus the presence of a small amount of Li$^+$ is insufficient for the precipitation of LiNbO$_3$ crystals [10].

At this moment, although the dissolution mechanism of LiNbO$_3$ crystals into TeO$_2$-based glasses has

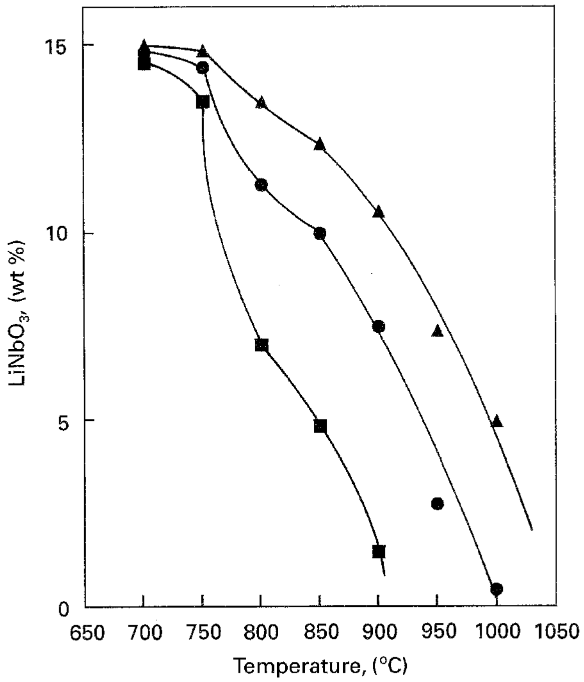

Figure 10 The remaining amounts of $LiNbO_3$ crystals after remelting at various temperatures and times in the mixture $80TeO_2$–$15Li_2O$–$5Nb_2O_5$ + 15 wt % $LiNbO_3$. (■) = 2 min, (●) = 1.5 min and (▲) = 1.0 min.

not been clarified, one possible explanation for the present results is to assume that the dissolution of Li^+ of the $LiNbO_3$ crystals into the TeO_2–Li_2O–Nb_2O_5 glasses is faster than that of Nb^{5+}. If so, the composition of the $LiNbO_3$ crystals changes gradually into Li^+ deficient $LiNbO_3$ crystals during remelting, and consequently Li^+ deficient $LiNbO_3$ crystals transform into the stable crystalline phase, i.e. $LiNb_3O_8$. Further, the dissolution rate of the Li^+ of the $LiNbO_3$ crystals into the TeO_2-based glasses would depend on the concentration of Li^+ in the TeO_2-based glasses. That is, in the TeO_2-based glasses with high Li^+ contents, the dissolution rate of the Li^+ of the $LiNbO_3$ crystals would decrease due to a small Li^+ concentration gradient between the crystals and the glasses, thus no Li^+ deficient $LiNbO_3$ crystals are produced and consequently no phase transformation of $LiNbO_3$ to $LiNb_3O_8$ occurs. It should be pointed out that many post-growth processing operations for $LiNbO_3$ single crystals involve as an important mechanism the diffusion of Li^+ through the $LiNbO_3$ crystals [11].

It is useful to discuss the structural features of $LiNbO_3$ and $LiNb_3O_8$. $LiNbO_3$ has a tendency to non-stoichiometry and hence with a ratio Li^+: $Nb^{5+} < 1$, meaning that $LiNbO_3$ has a very high concentration of intrinsic defects [12]. For optical device applications it is very important to control the ratio of Li^+: Nb^{5+} in $LiNbO_3$. Furthermore, it is well known that in $LiNbO_3$ the oxygen octahedra share faces along the c-axis and one third of the octahedral interstices are vacant [13]. On the other hand, in $LiNb_3O_8$ the oxygen octahedra share edges and half of the oxygen octahedral interstices are vacant [14]. Therefore, it is considered formally that the composition of $LiNb_3O_8$ corresponds to that of Li_2O depleted $LiNbO_3$. These structural features of $LiNbO_3$ and $LiNb_3O_8$ seem to support our dissolution mechanism stated above. Finally, it should be pointed out that $LiNb_3O_8$ grows on $LiNbO_3$ substrates at annealing temperatures up to 750 °C during Ti:$LiNbO_3$ optical waveguide fabrication, although the mechanism of formation of $LiNb_3O_8$ is still under discussion [15].

4.2. Transparency of $LiNbO_3$ incorporated glasses

It should be emphasized that the $80TeO_2$–$15Li_2O$–$5Nb_2O_5$ glasses containing about 7 wt % $LiNbO_3$ crystals with a diameter of 5–10 μm are transparent. Usually, for example, in order to obtain transparent bulk SiO_2-based glasses containing semiconductors such as CdS or $CdS_{1-x}Se_x$, the diameter of the semiconductor particles present in the glasses must be smaller than the wavelength of visible light, and their concentration is limited to around a few weight percent [16]. As discussed in the previous paper [1], it is considered that a small difference in the refractive indices between the matrix glass ($n = 2.07$) and $LiNbO_3$ crystals ($n = 2.296$) leads to only a small fraction of the light being reflected at the interface between them and this results in transparency, even though the particle size is much larger than the wavelength of visible light.

We now quantitatively consider the scattering loss of light at the glass/$LiNbO_3$ interface using the well-known Fresnel formula. If the incident angle is normal (90°), the fraction, R, of light reflected at the interface is estimated from the following equation.

$$R = \left(\frac{n_a - n_b}{n_a + n_b}\right)^2 \tag{1}$$

where n_a and n_b are the refractive indices of phases a and b, respectively. Firstly, let us estimate the scattering loss at the air/matrix glass or air/$LiNbO_3$ interface, because both the matrix glass and the $LiNbO_3$ crystals have values of the refractive index larger than 2.0. The transmittances, T, for the matrix glass itself and for pure $LiNbO_3$ single crystals are estimated using the Lambert–Beer law,

$$T = \frac{I_o}{I_i} = (1 - R)^2 e^{-\alpha x} \tag{2}$$

where I_i and I_o are the intensity of the incident and output light, respectively, α the absorption coefficient and x the sample thickness. For the air/glass and air/$LiNbO_3$ interfaces, the values of $(1 - R)^2$ are 0.77 and 0.71, respectively. As shown in Fig. 6, the transmittances at above $\lambda = 600$ nm are $T = 76\%$ for the matrix glass and $T = 70\%$ for the $LiNbO_3$ single crystals, indicating that the origin of the main scattering loss above $\lambda = 600$ nm in the TeO_2-based glasses and $LiNbO_3$ crystals is the scattering at the interface between air and glasses or crystals. This also means that the absorption of light above 600 nm in the matrix glass itself or $LiNbO_3$ single crystal itself is extremely small.

The above discussion indicates that the most important factor for the scattering loss of light in the

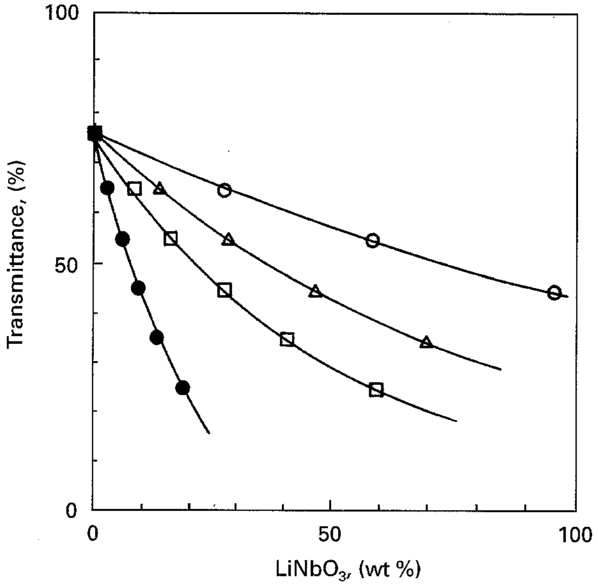

Figure 11 Calculated transmittances of the TeO$_2$-based glass ($n = 2.07$) containing various amounts of LiNbO$_3$ crystals with various thicknesses, d. (○): $d = 10\ \mu m$, (△) $d = 5\ \mu m$, (□) $d = 3\ \mu m$ and (●) $d = 1\ \mu m$.

TeO$_2$-based glasses containing LiNbO$_3$ crystals is the glass/LiNbO$_3$ interface. In other words, the total scattering loss of the light is determined by the number of the interfaces. When LiNbO$_3$ crystals with a thickness of d are arranged in a TeO$_2$-based glass with a thickness of L and the number of LiNbO$_3$ crystals is N, the intensity of output light is estimated from the following equation,

$$I_o = I_i(1 - R_g)^2(1 - R_c)^{2N}\exp[-(L - Nd)\alpha_g] \exp[-N_d\alpha_c] \quad (3)$$

where R_g and R_c are the fraction of light reflected at the air/glass and glass/LiNbO$_3$ interfaces, respectively, and α_g and α_c the absorption coefficients of a matrix glass and a LiNbO$_3$ crystal, respectively. As discussed above, it is reasonable to assume that the terms of $\exp[-(L - Nd)\alpha_g]$ and $\exp[-Nd\alpha_c]$ are almost unitary. Therefore, the reduction in the transmittance due to the incorporation of the LiNbO$_3$ crystals is estimated from the term of $(1 - R_c)^{2N}$, for example, $N = 29$ for a 10% reduction, $N = 44$ for a 15% reduction, a value of $T = 76\%$ is used as the transmittance in the original matrix glass containing no LiNbO$_3$ crystals. For a given concentration of LiNbO$_3$ crystals the reduction of transmittance is increased by decreasing the size of the LiNbO$_3$. That is, for the case of LiNbO$_3$ crystals with a small thickness, even a small amount will produce a large reduction of transmittance. Conversely, in the case of LiNbO$_3$ with a large thickness, even the glass containing a large amount of LiNbO$_3$ will have an excellent transparency. The relationship between the amount of LiNbO$_3$ crystals and the transmittance were calculated using the density values of the matrix glass (5.06 g cm^{-3}) and LiNbO$_3$ crystals (4.64 g cm^{-3}) for various thicknesses, d, and the results are shown in Fig. 11. It is seen from Fig. 11 that theoretically an incorporation of 15 wt % LiNbO$_3$ crystals with a thickness of 5 μm produces a reduction of only 10% in the transmittance. In the present study, we found from Fig. 6 that the glass containing about 3 wt % LiNbO$_3$ crystals with a diameter of 5–10 μm shows a reduction of 10% in the transmittance. This might indicate that LiNbO$_3$ crystals with small diameters are still included in the remelted sample. In conclusion, it is feasible to prepare highly transparent TeO$_2$-based glasses containing a large amount of LiNbO$_3$ crystals by controlling incorporation process.

5. Conclusions

The fabrication of transparent tellurite glasses containing LiNbO$_3$ crystals was tried using an incorporation method. The following results were obtained.

1. The dissolution behaviours of LiNbO$_3$ crystals (15 wt %) in the $80TeO_2–(20 - x)Li_2O–xNb_2O_5$ glasses depended greatly on the ratio of Li$_2$O : Nb$_2$O$_5$. In particular, when the LiNbO$_3$ crystals were dissolved and dispersed in the glass with Li$_2$O : Nb$_2$O$_5$ = 1, the crystals remaining in the glass after incorporation were LiNb$_3$O$_8$.
2. The favourite glass composition for the incorporation of LiNbO$_3$ crystals was 80TeO$_2$–15Li$_2$O–5Nb$_2$O$_5$. The maximum amount of LiNbO$_3$ crystals remaining in the transparent glass after incorporation was about 7 wt %.
3. A small difference in the refractive indices between the matrix glasses and the incorporated LiNbO$_3$ crystals is a significant reason for the observed transparency.

References

1. H. G. KIM, T. KOMATSU, R. SATO and K. MATUSITA, *J. Non-Cryst. Solids* **162** (1993) 201.
2. T. KOMATSU, K. SHIOYA and K. MATUSITA, *J. Am. Ceram. Soc.* **76** (1993) 2923.
3. T. KOMATSU, H. TAWARAYAMA, H. MOHRI and K. MATUSITA, *J. Non-Cryst. Solids* **135** (1991) 105.
4. T. KOMATSU, H. TAWARAYAMA and K. MATUSITA, *J. Ceram. Soc. Japan* **101** (1993) 48.
5. J. E. STANWORTH, *J. Soc. Glass Technol.* **36** (1952) 217.
6. A. K. YAKHKIND, *J. Am. Ceram. Soc.* **49** (1966) 670.
7. H. NASU, O. MATSUSHITA, K. KAMIYA, H. KOBAYASHI and K. KUBODERA, *J. Non-Cryst. Solids* **124** (1990) 275.
8. S. H. KIM, T. YOKO and S. SAKKA, *J. Am. Ceram. Soc.* **76** (1993) 865.
9. K. NASSAU, H. J. LEVINSTEIN and G. M. LOIACONO, *J. Phys. Chem. Solids* **27** (1966) 989.
10. P. LERNER, C. LEGRAS and J. P. DUMAN, *J. Cryst. Growth* **3** (1968) 231.
11. D. H. JUNDT, M. M. FEJER, R. G. NORWOOD and P. F. BORDUI, *J. Appl. Phys.* **72** (1992) 3468.
12. O. F. SCHIRMER, O. THIEMANN and M. WOHLECKE, *J. Phys. Chem. Solids* **52** (1991) 185.
13. M. M. ABOUELLEIL and F. L. LEONBERGER, *J. Am. Ceram. Soc.* **72** (1989) 1311.
14. B. M. GATEHOUSE and P. LEVERETT, *Cryst. Struct. Comm.* **1** (1972) 83.
15. M. N. ARMENISE, C. CANALI, M. DE SARIO, A. CARNERA, P. MAZZOLDI and G. CELOTTI, *J. Appl. Phys.* **54** (1983) 6223.
16. N. F. BORRELLI, D. W. HALL, H. J. HOLLAND and D. W. SMITH, *ibid.* **61** (1987) 5399.

Received 2 September 1994
and accepted 17 October 1995